AD 296 973

UNCLASSIFIED

29 6973

TRG

CATALOGED BY ASTIA
AS AD No.

296 973

TECHNICAL RESEARCH GROUP
400 BORDER STREET • EAST BOSTON • MASS.

AFCRL-62-950

APPLICATION OF FRESNEL ZONE THEORY TO MICROWAVE ANTENNA DESIGN

by
Alan F. Kay

Scientific Report Number 3
Contract Number AF19(604)-8057

AFCRL-62-950

APPLICATION OF FRESNEL ZONE THEORY TO MICROWAVE ANTENNA DESIGN

by

Alan F. Kay

TRG, Incorporated
400 Border Street
East Boston 28, Massachusetts

Contract Number AF19(604)-8057
Project Number 151
Scientific Report Number 3

November 15, 1962

Project 4600
Task 460002

PREPARED FOR

ELECTRONICS RESEARCH DIRECTORATE
AIR FORCE CAMBRIDGE RESEARCH LABORATORIES
OFFICE OF AEROSPACE RESEARCH
UNITED STATES AIR FORCE
BEDFORD, MASSACHUSETTS

Requests for additional copies by Agencies of the Department of Defense, their contractors, and other Government agencies should be directed to the:

ARMED SERVICES TECHNICAL INFORMATION AGENCY
ARLINGTON HALL STATION
ARLINGTON 12, VIRGINIA

Department of Defense contractors must be established for ASTIA services or have their "need-to-know" certified by the cognizant military agency of their project or contract.

All other persons and organizations should apply to the:

U.S. DEPARTMENT OF COMMERCE
OFFICE OF TECHNICAL SERVICES
WASHINGTON 25, D. C.

TABLE OF CONTENTS

LIST OF FIGURES

ABSTRACT

Some fundamental formulas are derived which are corrections to geometrical optics for radiation from bounded wavefronts. These formulas apply in both the near and far field, in focal and caustic regions, and in lit, twilight, and dark zones. Applications are made to improving the gain of a spherical reflector and the analysis of (generally unwanted) focussing of spillover energy in microwave systems.

Earlier applications were in the design of low noise feeds and line source feeds for spherical reflectors.

I - INTRODUCTION

Geometrical optics is commonly used in the design of microwave antennas. The parabolic reflector, the microwave lens, the shaped beam reflector, are but a few of the common applications. Geometrical optics is often alleged to be accurate in these applications provided the characteristic dimensions of the reflector or lens are large compared to the wavelength or depending on the particular situation, if one is not too close to a focal region, a caustic, a shadow boundary, or if one is or is not in the "far field."

The author has previously considered two antenna design problems, wherein geometrical optics was an important guide, but not sufficiently accurate to obtain essential design information. These were (a) design of a line source feed for a spherical reflector [1] and (b) design of horns for high aperture efficiency, low spillover, and broad bandwidth [2]. In both cases physical optics considerations did prove sufficiently precise for all practical needs. However, also, relatively simple corrections to geometrical optics proved as satisfactory as physical optics and very helpful for obtaining physical insight.

It turns out that properly applied these corrections often permit use of geometrical optics with reasonable accuracy for dimensions down to one wavelength or in focal or caustic regions.

The correction terms sought are not essentially different from those considered by Keller and others [3] at NYU but we are concerned directly with situations which arise in the design of microwave feeds and antennas.

One purpose of this report is to present some practical examples.

Geometrical optics deals with rays and wavefronts. The field strength and phase at any point can be obtained from the path length from the source to the point along the ray or rays which pass through the point. Similarly the amplitude of the field is associated with the density of the rays near the point. No difficulty with this picture generally arises as long as the wavefronts have no boundaries, i.e. are either infinite or are closed. However, as soon as a finite reflector, aperture, or a finite distributed source is introduced into the picture, one is dealing with "pieces" of wavefronts which are bounded in the sense that the field is usually and properly assumed to terminate abruptly at the boundary.

It is perhaps surprising that the assumption that the field vanishes or satisfies some simple impedance condition in a boundary plane outside the aperture of a horn in free space or outside of the reflector surface of a paraboloid is not a bad one. For practical purposes one need not look for the edge currents which are actually flowing in the boundary structure to provide correction terms to geometrical optics. To see where the correction terms to geometrical optics arise from consider the general physical optics formula for the field at a point P ahead of a wavefront in terms of a surface integral over the wavefront as given, for example, by eq(43), p. 119 of [4]:

(1) $$u_p = \frac{j}{2\lambda} \int_S \frac{u(1 + \cos \phi)}{r} e^{-jkr} dS$$

where ϕ is the angle between $\bar{n}$, the outward normal of the wavefront **S**, and $\bar{r}$ the vector of length r from the integration point to the observation point **P**,

u is the field over S and $k = 2\pi/\lambda$. The wavefront S may be a closed surface or, the more common case in microwave optics, an open surface, such as the front surface of a reflector or the aperture of a horn, lens, reflector, or array, i.e. a surface having a boundary. The geometrical optics theorems can be obtained from the stationary phase approximation applied to (1) as is done in reference [4] in the pages following p. 119. Several assumptions are necessary for these approximations. The most basic of these is usually stated as the necessity for k large. When the area of integration is an open surface with a boundary a more accurate formulation of this assumption is that there should occur a large number of phase cycles of the exponential in (1) as the integration point varies from the stationary phase point to any boundary point. The location of the stationary phase point(s) is (are) readily determined as the point(s) in which the ray(s) through P intersect the wavefront S. S can be thousands of wavelengths across, k can correspond to optical frequencies, and the stationary phase approximation can be very poor. The most common example occurs if r is almost constant over S i.e. P is in a focal region. Another common failure occurs if the amplitude distribution varies appreciably near the stationary phase point. An important example of this is given in Section 4.

A simple way to visualize these effects is by the use of Fresnel zones. With a little practice Fresnel zones are almost as easy to visualize as rays and wavefronts and are of considerable help.

Fresnel zones are nested zones on a wavefront which surround a stationary phase point. They of course depend on the particular wavefront in question, but also they depend on the observation point. There is also a different set of Fresnel zones for each stationary phase point. More explicitly the nth Fresnel zone is defined as the region of the wavefront for which

$$(n - 1)\pi < |k(r-p)| < n\pi, \tag{2}$$

where p is the distance from P to the stationary phase point, i. e, the point where the ray through P intersects the wavefront.

The first Fresnel zone contains all points on the wavefront immediately surrounding the stationary phase point which add constructively with the contribution to P of the stationary phase point. The second Fresnel zone contains all points of the wavefront immediately surrounding the first Fresnel zone which subtract or add destructively to the contribution from the first Fresnel zone - and so on. It is convenient therefore to think of the first Fresnel zone as "+", the second "-", etc. If one is looking for gain at P, it is not a bad idea to think of the first Fresnel zone as "good," the second as "bad," etc.

If the integrands are slowly varying, the contributions at P of the different Fresnel zones are roughly proportional to their area. When the wavefront has a boundary, some of the Fresnel zones will be intersected by or "cut" the boundary and their area is accordingly diminished. The part of the Fresnel zone inside of the boundary is called the "illuminated" part.

If the first Fresnel zone cuts the boundary, the observation point P is said to be in the twilight zone. If the first Fresnel zone is entirely outside of the boundary, P is in the dark zone, if entirely inside of the boundary (i.e. entirely illuminated), P is in the lit zone. If the stationary phase point is exactly on the boundary so that the first Fresnel zone is usually about half illuminated, P is on the shadow boundary. If there is more than one stationary phase point, these definitions apply with respect to each stationary phase point; the relative regions of one may have no relation to those of the other. (See Fig. 1).

II - DERIVATION OF FUNDAMENTAL FORMULAS

Any rectangular component of the E or H field at a point P inside a free space region bounded by any smooth closed surface S may be expressed by the Huygens-Green relation as an integral over S as follows:

$$u_p = \frac{1}{4\pi}\int_S \frac{e^{-jkr}}{r}\left[u\left(jk + \frac{1}{r}\right)\cos\phi - \frac{\partial u}{\partial n}\right]dS \tag{3}$$

(eq(5), p. 109, [4]), where u, k, r, and ϕ are as previously defined.

If on the surface S a geometrical optics description of the field is valid, we may write u on S as

$$u = |u|e^{-jk\psi} \tag{4}$$

where ψ is a phase function satisfying

$$|\nabla\psi| = 1 \quad [4, \text{p. } 115]. \tag{5}$$

SHADED AREAS = ODD FRESNEL ZONES.
PLAIN AREAS = EVEN FRESNEL ZONES.

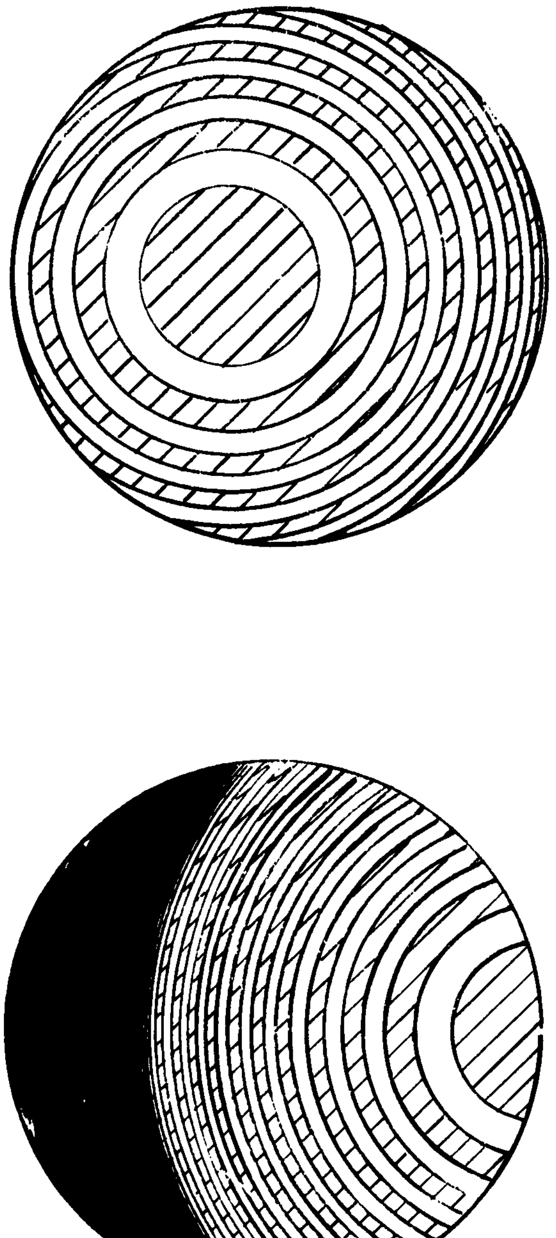

BOUNDARY SUFFICIENTLY FAR FROM STATIONARY PHASE POINT O SO THAT GEOMETRICAL APPROXIMATION IS GOOD.

BOUNDARY CUTS FIRST FRESNEL ZONE SMOOTHLY AT STATIONARY PHASE POINT; THEREFORE OBSERVATION POINT IS ON SHADOW BOUNDARY AND EFFECT OF BOUNDARY IS TO LOWER FIELD 6 db.

FIG. 1

EXAMPLES OF FRESNEL ZONES

If the relative change in the amplitude $|u|$ is small compared to unity over a wavelength distance, we may write

(6) $$\frac{\partial u}{\partial n} = -jku\nabla\psi \cdot \bar{n} = jku \cos \alpha$$

where α is the angle between the outward normals to the wavefront and to the surface S Furthermore if the observation point P is several wavelengths from S, the term jk is much larger than $1/r$ in (3) and (3) may be written approximately as

(7) $$u_P = \frac{j}{2\lambda} \int_S \frac{ue^{-jkr}}{r} (\cos \alpha + \cos \phi) dS.$$

We note that (7) is the generalization of (1) when S is not necessarily a wavefront, but any surface The only assumption used to obtain (7), it should be noted, is that the field has a geometrical optics behavior on S, but not necessarily inside or outside of S, and that P is several wavelengths from S.

Let us assume that S is a wavefront and that there is one stationary phase point, O, on S with respect to P.

Let us introduce a Cartesian coordinate system with the negative z axis along $\bar{n}$ at 0. Let the surface S be smooth at O, so that by suitable choice of x and y axes, the equation for the surface may be written in the neighborhood of O as

$$z = \frac{x^2}{2R_1} + \frac{y^2}{2R_2} + \ldots \tag{8}$$

where R_1 and R_2 are the principal radii of curvature at O. Then to first order in x^2 and y^2

$$r = \sqrt{x^2 + y^2 + (z+p)^2} \cong p + \frac{\alpha x^2 + \beta y^2}{2} + \ldots \tag{9}$$

where

$$\alpha = \frac{R_1 + p}{R_1 p}, \quad \beta = \frac{R_2 + p}{R_2 p} \quad . \tag{10}$$

We may therefore, write (1) as

$$u_P = \frac{je^{-jkp}}{2\lambda} \int_S \frac{u(1 + \cos \phi)}{r} e^{-\frac{jk}{2}(\alpha x^2 + \beta y^2)} dx\, dy \tag{11}$$

where in order to retain only the leading terms in (8) and (9), we must assume either that (a) the only important contribution to the integral comes from the neighborhood of O or (b) that the principal curvatures R_1 and R_2 describe S well over the area where the contribution to the integral is significant.

At this point we shall assume that S is bounded by curves parallel to the Fresnel zone boundaries. This treats a case of considerable interest and also, in a sense to be considered later, gives upper and lower bounds for the field values for more general boundary curves. To be explicit let us make the change of variables in (11) from x, y to ρ, θ defined by

$$\rho \cos\theta = \sqrt{\frac{k\alpha}{2}}\, x, \qquad \rho \sin\theta = \sqrt{\frac{k\beta}{2}}\, y, \tag{12}$$

where the surface is defined by

$$\rho_1 \leq \rho \leq \rho_2, \quad \rho \text{ on } \mathbf{S}. \tag{13}$$

Since

$$\frac{k}{2}\sqrt{\alpha\beta}\, dx\, dy = \rho\, d\rho\, d\theta \tag{14}$$

we may write (11) as

$$u_P = \frac{2je^{-jkp}}{p\sqrt{\alpha\beta}} \int_{\rho_1}^{\rho_2} e^{-j\rho^2} u_1(\rho)\rho\, d\rho \tag{15}$$

where $u_1(\rho)$ is a "weighted" illumination, averaged with respect to θ, defined by

$$u_1(\rho) = \frac{1}{2\pi} \int_0^{2\pi} \frac{u(\rho, \theta)\left(\frac{1 + \cos\phi}{2}\right)}{\left(\frac{r}{p}\right)}\, d\theta, \tag{16}$$

with the property that

(17) $$u_1(0) = u(0, \theta) = u(0).$$

(a) Gain

In particular, if the observation point distance p is large compared to the diameter of the wavefront, and if the total curvature of the wavefront is not excessive then

(18) $$\frac{r}{p} \simeq 1, \quad \frac{1 + \cos \phi}{2} \simeq 1$$

and, in this case, $u_1(\rho)$ is the illumination averaged with respect to the angle θ.

(18a) $$u_1(\rho) = \frac{1}{2\pi} \int_0^{2\pi} u(\rho, \theta) d\theta.$$

A quantity of considerable interest is the gain G at P which may be defined as the ratio of the power density at P to that which would prevail if all of the power flowing through S were radiated isotropically from the stationary phase point. Under the assumption that (18) holds, the gain is given by

(19) $$G = \frac{|u_P|^2}{\left(\int_S |u|^2 dx\, dy \Big/ 4\pi p^2\right)}.$$

Using (14) and (15) and employing the fact that the area A of the wave front S: $\rho_1 \leq \rho \leq \rho_2$ is given by

$$A = \iint_S dx\,dy = \frac{2}{k\sqrt{\alpha}} \int_0^{2\pi} \int_{\rho_1}^{\rho_2} \rho\, d\rho\, d\theta = \frac{\lambda(\rho_2^2 - \rho_1^2)}{\sqrt{\alpha\beta}} \tag{20}$$

we may write (19) as

$$G = \frac{4A \left| \int_{\rho_1}^{\rho_2} \int_0^{2\pi} e^{-j\rho^2} u(\rho,\theta) \rho\, d\rho\, d\theta \right|^2}{\lambda^2(\rho_2^2 - \rho_1^2) \int_{\rho_1}^{\rho_2} \int_0^{2\pi} u^2(\rho,\theta)\rho\, d\rho\, d\theta} \,. \tag{21}$$

As a check, observe that if $u(\rho,\theta)$ is constant and $\rho_2^2 << \pi$, then (21) reduces to the well known formula for maximum gain for a uniformly illuminated aperture

$$G = \frac{4\pi A}{\lambda^2}. \tag{22}$$

In the more general case it is of interest to determine what real function $u(\rho,\theta)$ maximizes G. The physical application arises with a microwave optical system which produces imperfect focussing fed by a point source feed whose primary pattern should be selected in so far as possible to maximize gain. The mathematical problem is solved exactly in the Appendix, where it is shown that at least a 50% aperture efficiency may be achieved with the optimum illumination. By contrast if u is constant over the first Fresnel zone and zero elsewhere, the aperture efficiency is $4/\pi^2 = 40.6\%$, and if u is a Gaussian, of the form

$$u(\rho,\theta) = e^{-b\rho^2} \tag{23}$$

the optimum value of b for gain is unity (27.6db taper at the edge of the first Fresnel zone) and the aperture efficiency is merely 16%. (See also, Appendix, p. A4).

(b) Slowly Varying Illumination

An important special case occurs if the variation of the illumination function $u_1(\rho)$ in (15) is small per cycle of the exponential.

First let us integrate (15) by parts

(24) $$u_P = \frac{e^{-jkp}}{p\sqrt{\alpha\beta}}\left(e^{-j\rho_1^2}u_1(\rho_1) - e^{-j\rho_2^2}u_1(\rho_2) + \int_{\rho_1}^{\rho_2} e^{-j\rho^2}\frac{\partial u_1(\rho)}{\partial\rho}\,d\rho\right).$$

as As $k \to \infty$, the integral term in (24) is of order $1/\sqrt{k}$, whereas the integrated terms are of order unity. In any case, if the percentage variation of $u_1(\rho)$ is small per cycle of the exponential, the integral term in (24) may be neglected, to obtain the approximation

(25) $$u_P = \frac{e^{-jkp}}{p\sqrt{\alpha\beta}}\left(e^{-j\rho_1^2}u_1(\rho_1) - e^{-j\rho_2^2}u_1(\rho_2)\right).$$

The basic equation from which the principal theorems of geometrical optics may be derived is a special case of this formula: $\rho_1 = 0$, $\rho_2 = \infty$. This corresponds to the case of a closed or infinite wavefront with no boundary, i.e., no diffraction. If there are no sources at ∞, $u_1(\infty) = 0$, and from (10) and (17),

(26) $$u_P = u(0)e^{-jkp}\sqrt{\frac{R_1R_2}{(R_1+p)(R_2+p)}} \quad \Big\{ \; S, \text{ unbounded}.$$

Eq(26) is the same as eq(51), p 122 of [1], and is used in [1] to derive the theorems of geometrical optics

If the wavefront is open, contains the stationary phase point and has a single boundary curve $\rho = \rho_2$ parallel to a Fresnel zone boundary, the correct formula to use is eq(25) with $\rho_1 = 0$

$$(27) \qquad u_P = (u(0) - e^{-j\rho_2^2} u_1(\rho_2)) e^{-jkp} \sqrt{\frac{R_1 R_2}{(R_1 + p)(R_2 + p)}} \qquad \left\{ \begin{array}{l} \text{S contains} \\ \text{stationary phase} \\ \text{point, has single} \\ \text{boundary } \rho = \rho_2 \end{array} \right.$$

Similarly, if the wavefront has a single boundary curve $\rho = \rho_1$ but does not contain the stationary phase point, the correct formula is obtained by setting $\rho_2 = \infty$:

$$(28) \qquad u_P = e^{-j\rho_1^2} u_1(\rho_1) e^{-jkp} \sqrt{\frac{R_1 R_2}{(R_1 + p)(R_2 + p)}} \qquad \left\{ \begin{array}{l} \text{S excludes} \\ \text{stationary phase} \\ \text{point, has single} \\ \text{boundary } \rho = \rho_1 \end{array} \right.$$

The latter is of interest in calculating the effects of spillover (see Section V).

An important special case of (27) occurs when S consists of a small number of Fresnel zones By the assumption that the variation of $u_1(\rho)$ is small per cycle, we have approximately that if S has an odd number $(2n + 1)$ of Fresnel zones, (27) becomes

$$(29) \qquad u_P = 2u(0) e^{-jkp} \sqrt{\frac{R_1 R_2}{(R_1 + p)(R_2 + p)}} \qquad \left\{ \begin{array}{l} \text{S contains first} \\ \text{(2n+1) Fresnel zones,} \\ \text{n, small} \end{array} \right.$$

If S has an even number (2n) of Fresnel zones, (27) is approximately zero. From (29) and (27) we see that.

If the percentage field variation is small over the first N Fresnel zones of an observation point P, the field at P is approximately doubled or made to vanish when the wavefront is blocked or "stopped down" to the area of these N Fresnel zones, depending on whether N is odd or even, respectively.

Another way to attempt to increase the field strength at P is to focus the energy to P. If all of the energy over an area A of the wavefront were focussed with respect to P by some means which need not be specified, the phase factor in the integral in (15) would be suppressed. If then only A were illuminated (15) could be written as

$$u_P = \frac{j u_{av} A e^{-jkp}}{p\lambda} \tag{30}$$

where u_{av} is the average weighted illumination over A as defined by

$$u_{av} = \frac{1}{A} \int_A \frac{u\left(\frac{1+\cos\phi}{2}\right)}{\left(\frac{r}{p}\right)} dA. \tag{31}$$

From (10) and (20), the area of the first N Fresnel zones is

$$A_N = N\pi\lambda p \sqrt{\frac{R_1 R_2}{(R_1 + p)(R_2 + p)}} \quad . \tag{32}$$

In this case (30) becomes

$$u_P = jN\pi u_{av} e^{-jkp} \sqrt{\frac{R_1 R_2}{(R_1 + p)(R_2 + p)}} \quad \left\{ \begin{array}{l} \text{First N Fresnel zones} \\ \text{focussed, other blocked.} \end{array} \right. \tag{33}$$

so that, if the percentage field variation is small over the first N Fresnel zones of an observation point P, the field strength at P is increased by $N\pi$, when the first N Fresnel zones are focussed to P and the remaining zones are blocked.

III - DETERMINATION OF THE TWILIGHT ZONE

If an observation point P in front of a bounded wave front lies on the edge ray or shadow boundary, the first few Fresnel zones are about one half of their normal size (Figure 1). The field at P is then about one half of its value (-6db) compared to an unbounded wave front with the same strength in the neighborhood of the stationary phase point O. Consider the locus of points L_b on the lit side of the shadow boundary so that the first Fresnel zone is interior to and just tangent to the aperture boundary; and in a similar fashion, the locus of points L_d on the dark side of the shadow boundary so that the first Fresnel zone is exterior to and just tangent to the aperture boundary (Figure 2).

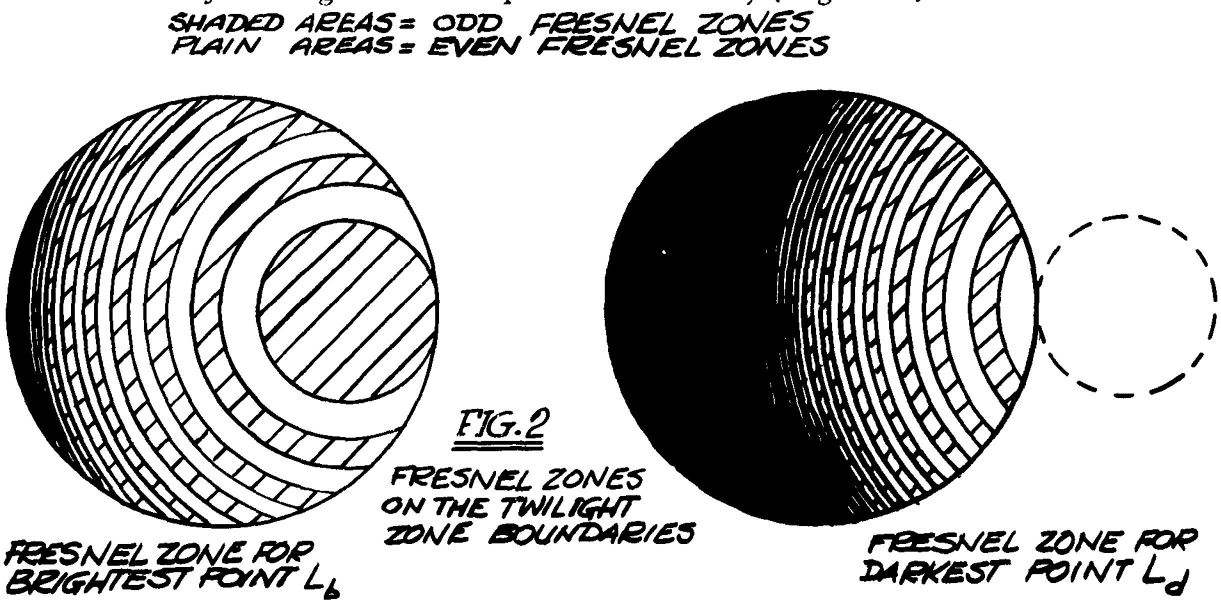

FIG. 2
FRESNEL ZONES ON THE TWILIGHT ZONE BOUNDARIES

Suppose we consider the case where the field u over the first few Fresnel zones is not too far from uniform. Then the contribution at P of the Fresnel zones are roughly proportional to their area. The points L_b are locally somewhat brighter since the odd Fresnel zones are suppressed by the boundary somewhat more than the even zones. Similarly L_d is somewhat darker locally. As one moves across a shadow boundary starting from the lit side the field amplitude and phase has ripples with the last and largest peak at L_b just before the shadow boundary or -6db point. The field in the dark zone also has ripples with the first and lowest relative minimum at L_d. This behavior is illustrated in Figure 3. It is a generalization of the well-known Fresnel integral patterns for the near field of a uniformly illuminated, linear aperture.

The region between L_b and L_d is called the "twilight zone."

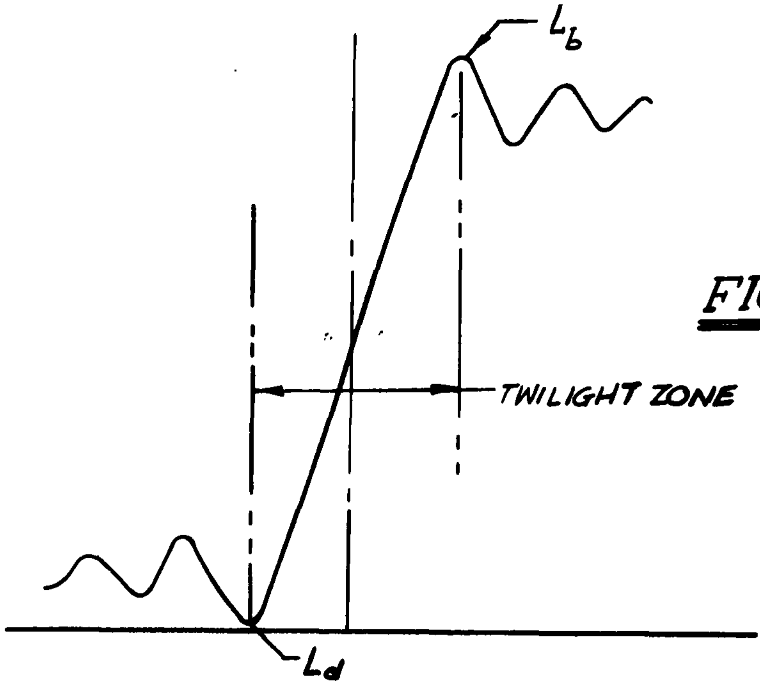

FIG. 3

The boundary curves of the twilight zone are hyperbolas which may be readily determined as follows. Let P_b be a point with polar coordinates (r, θ) on the locus L_b. Let the stationary phase point be O and let the boundary point on the first Fresnel zone be B. Let R_1 be the radius of curvature of the wavefront in the plane $\overline{P_b OB}$. Let the origin of coordinates be the center of curvature of the wavefront at O.

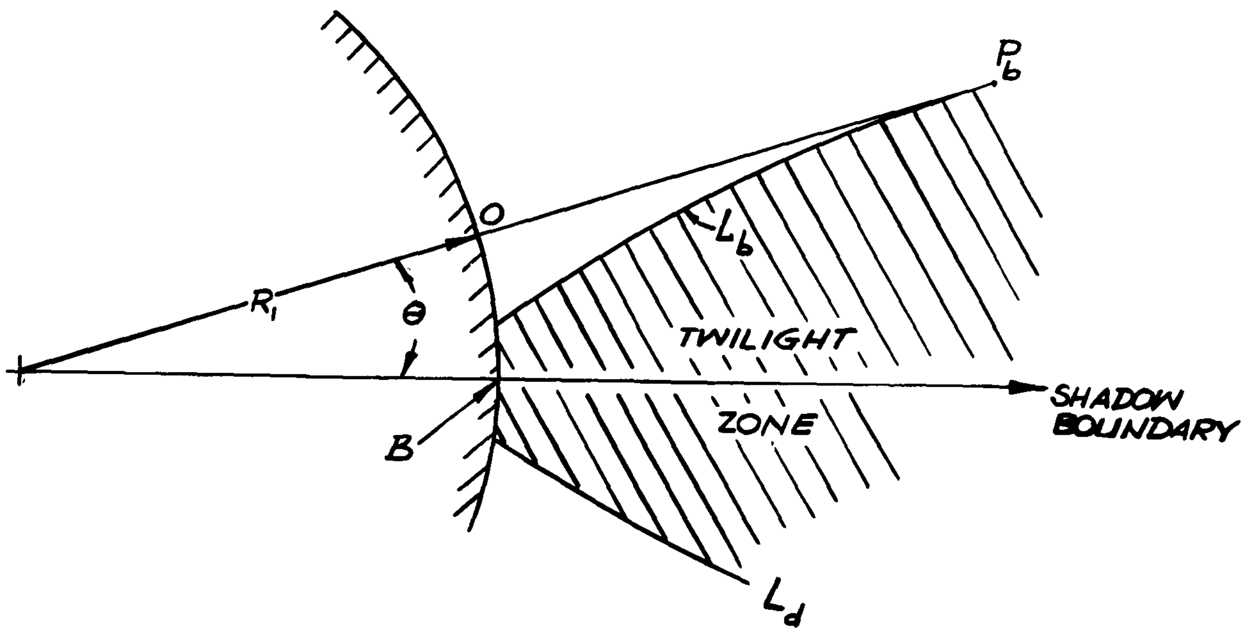

FIG. 4
LOCUS OF THE TWILIGHT ZONE

The condition which defines P_b as lying on L_b is

$$\overline{P_bB} = p + \frac{\lambda}{2}, \quad r = p + R_1 \tag{34}$$

where

$$\overline{P_bB} = \sqrt{r^2 + R_1^2 - 2R_1 r \cos\theta} \; . \tag{35}$$

The locus L_b is thus given by

$$r(\lambda - 2R_1(1 - \cos\theta)) = \lambda R_1 - \frac{\lambda^2}{4} \; . \tag{36}$$

This is an even function of θ. Negative values of θ actually give L_d, so that the twilight zone is symmetric about the shadow boundary. Equation (36) is a hyperbola which passes through the point $r = R_1$, $\theta = \cos^{-1}(1 - \frac{\lambda^2}{8R_1^2})$, on the wavefront and is asymptotic to the ray $\theta = \cos^{-1}(1 - \frac{\lambda}{2R_1})$. If $R_1 >> \lambda$, an approximate form of (36) is

$$\theta = \sqrt{\frac{\lambda(r - R_1)}{rR_1}} \; . \tag{37}$$

IV - GAIN OF A SPHERICAL REFLECTOR

(a) Point Source Feed

An application of the ideas developed in the preceding sections may be made to the analysis of a spherical reflector. Suppose at first a point source P is located at a distance ℓ from the center of a spherical reflector of radius $R > \ell$. Let the equation of the sphere in cylindrical coordinates be

$$z^2 + r^2 = R^2 \tag{38}$$

with z axis along $\overline{OP}$. After reflection the phase at a point at polar distance r in a plane perpendicular to $\overline{OP}$, relative to the phase at $r = 0$ is given by

$$\Delta_0 = \sqrt{R^2 + \ell^2 - 2\ell z} - 2R + z + \ell \quad , \qquad z = \sqrt{R^2 - r^2} \; . \tag{39}$$

This function is plotted in Figure 5 for several values of ℓ. As is well-known, the point P at $\ell = R/2$, the "paraxial focus," produces optimum focussing (flattest phase front) for small values of r.

The first Fresnel zone, in this case, occupies a circle of radius r' obtained by equating Δ_0 in (22) to $-\lambda/2$ and ℓ to $R/2$. The result is given by

$$r' = \sqrt{\lambda R\left(1 + \sqrt{\frac{3}{4} + \frac{2R}{\lambda}}\right) + \frac{\lambda^2}{4}\left(1 + \sqrt{\frac{3}{4} + \frac{2R}{\lambda}}\right)^2} \tag{40}$$

which, if $R >> \lambda$, is approximated by

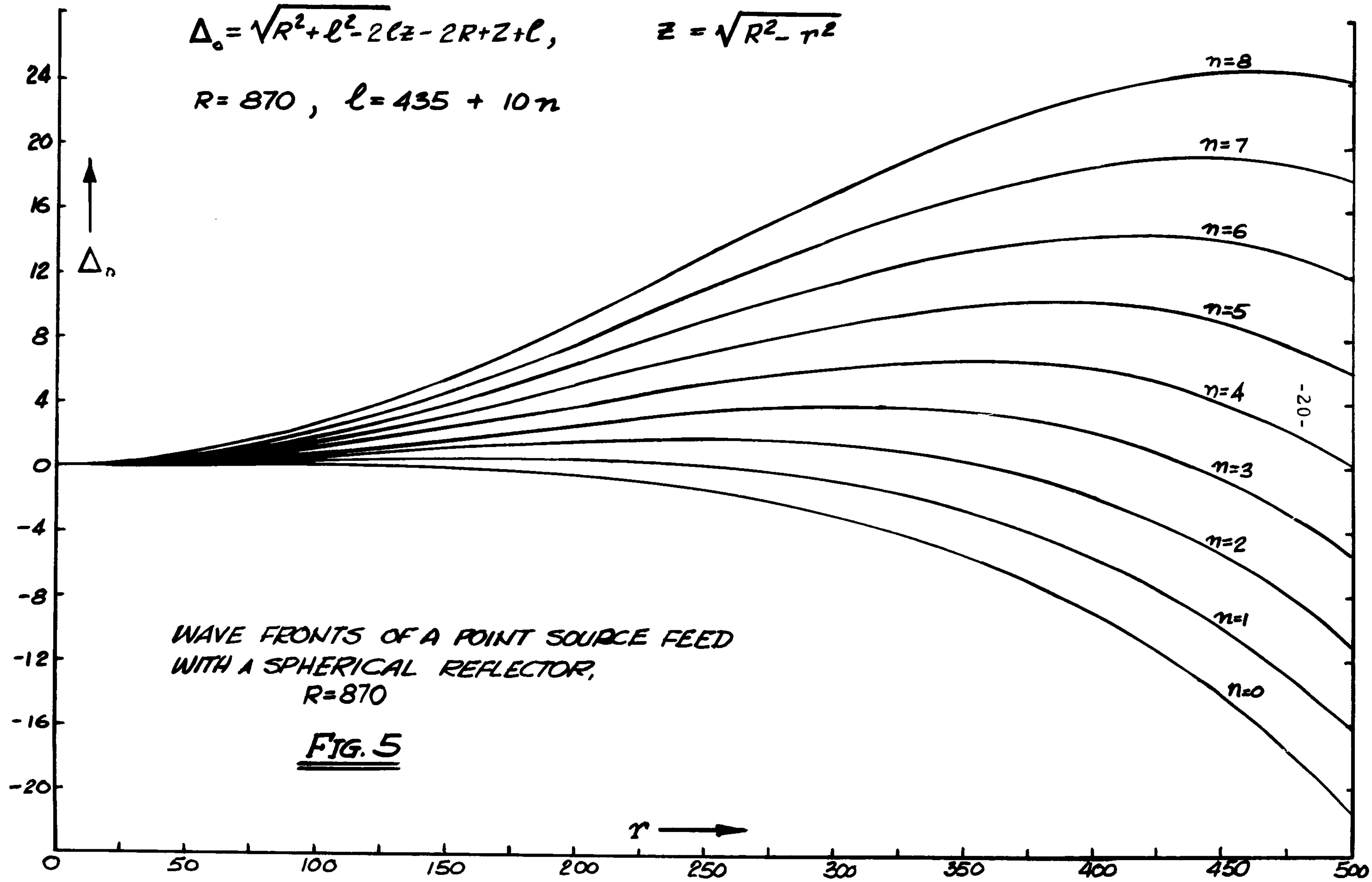

WAVE FRONTS OF A POINT SOURCE FEED WITH A SPHERICAL REFLECTOR, R=870

FIG. 5

$$r' \simeq (2\lambda)^{1/4} R^{3/4}. \tag{41}$$

If the physical reflector is of such radius r_1 at the aperture that $r' << r_1$, then maximum gain is obtained approximately when only the first Fresnel zone is illuminated. Assume then that the primary amplitude pattern is such that a 50% aperture efficiency is obtained over the first Fresnel zone. This may be achieved by the illuminations described in the Appendix.* Then

$$G_{r'} = \frac{1}{2}\left(\frac{2\pi r'}{\lambda}\right)^2 = \frac{2\pi^2 r'^2}{\lambda^2} \simeq 27.9\left(\frac{R}{\lambda}\right)^{3/2} \qquad R >> \lambda. \tag{42}$$

If, on the other hand, the source is located somewhat closer to the reflector, the area of the first Fresnel zone can be made larger. This area is maximized with respect to ℓ when the maximum of Δ_0 with respect to r has a value of $\lambda/2$. In this case the first Fresnel zone has a radius r'' which is the value of r (other than $r = 0$) at which $\Delta_0 = 0$. The maximum occurs at

$$r = R\sqrt{1 - \left(\frac{R}{2\ell}\right)^2} \tag{43}$$

---

* Strictly speaking, the assumption of fixed radii of curvature describing the wavefront near the first few Fresnel zones does not hold in this case. It is thought that no serious error is introduced thereby in this case, in the consideration of optimum gain. The optimum illuminations, however, may be appreciably different from those described in the Appendix.

and the optimum ℓ is

$$\ell = \frac{\lambda + 4R + \sqrt{\lambda^2 + 8\lambda R}}{8} \simeq \frac{R}{2} + \sqrt{\frac{\lambda R}{8}}\,, \quad \lambda << R \tag{44}$$

and the radius of the first Fresnel zone is

$$r'' = \sqrt{\lambda R\left(1 + \sqrt{1 + \frac{8R}{\lambda}}\right) + \frac{\lambda^2}{4}\left(1 + \sqrt{1 + \frac{8R}{\lambda}}\right)^2} \tag{45}$$

$$\simeq (8\lambda)^{1/4} R^{3/4} = \sqrt{2}\, r'.$$

Hence if $r'' < r_1$ and the point source is optimally located a distance ℓ given by (44) from the center of the sphere, the peak far field gain is approximately

$$G_{r''} = 2G_{r'} \simeq 55.8\left(\frac{R}{\lambda}\right)^{3/2}, \qquad R >> \lambda. \tag{46}$$

These expressions are plotted in Figure 6 for the dimension of the radio telescope at Arecibo, Puerto Rico: R = 870', r_1 = 500'. Other examples of interest are

f	R	$G_{r'}$, db	$G_{r''}$, db	G_L
40 kmc	2.5'	45.67	48.67	40
11 kmc	5'	41.78	44.78	38

The gain values G_L in the last column are quoted from ref[5].* It appears that these are several db below what they could be. Such low values

* Experimental results.

$$G_{\gamma'} = 10 \log_{10}\left[55.8\left(\frac{870}{\lambda}\right)^{3/2}\right]$$

$$G_{\gamma''} = G_{\gamma'} + 3\,db$$

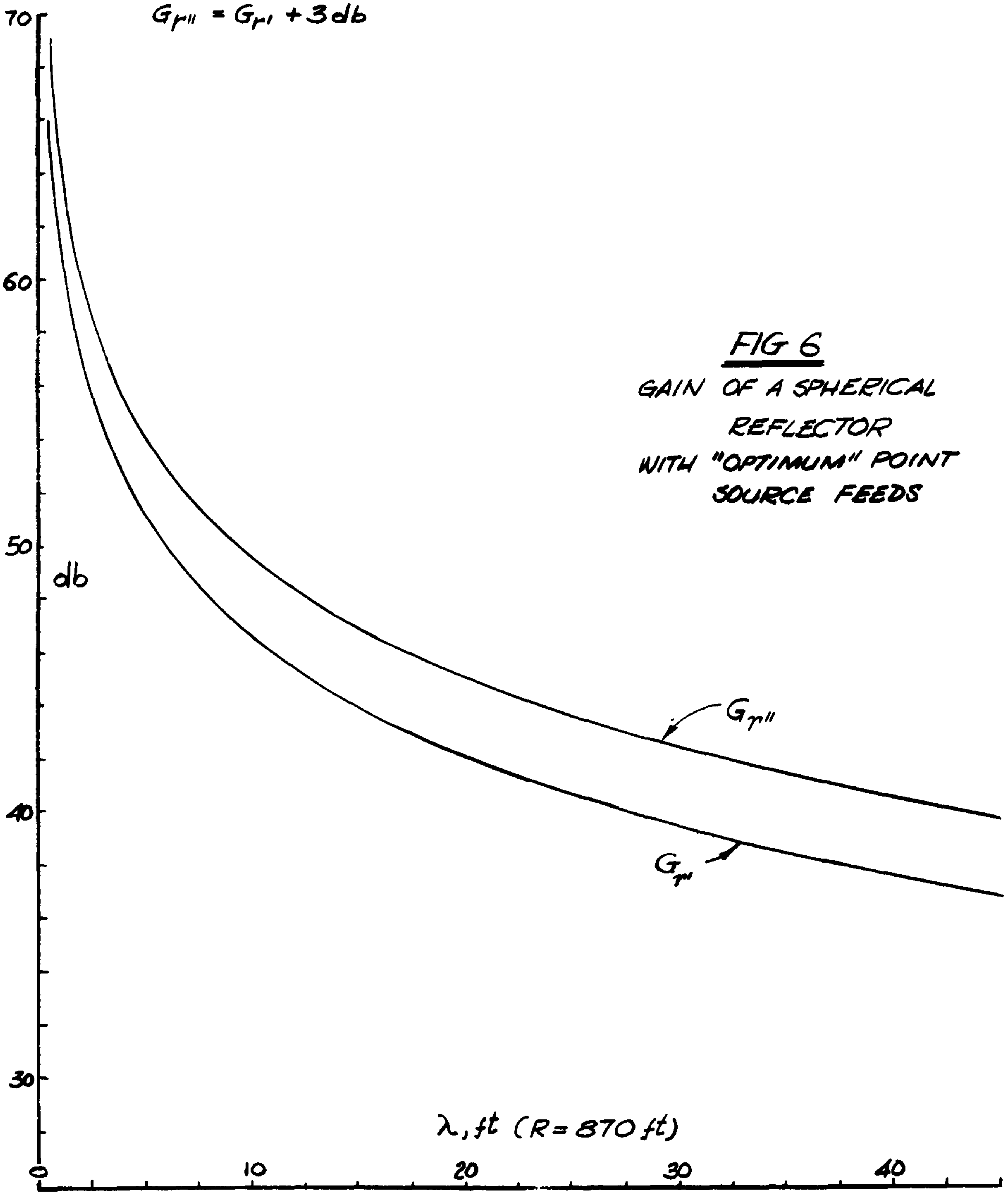

FIG 6

GAIN OF A SPHERICAL REFLECTOR WITH "OPTIMUM" POINT SOURCE FEEDS could be obtained if the feed illuminated two or three Fresnel zones or was not near an optimum taper. For example, as shown on p. 12 an optimum Gaussian feed pattern would have almost 5db less gain than the listed values for $G_{r'}$ and $G_{r''}$.

(b) Wide Flare Feed

If we use a large conical feed with flare length r_0 and vertex angle θ_0, it has been determined [2] that to first approximation, the phase front is a spherical cap in the lit region (Figure 7) with phase center at the vertex. In the twilight zone, the phase is determined by the path length $\overline{ABC}$ in Figure 7.

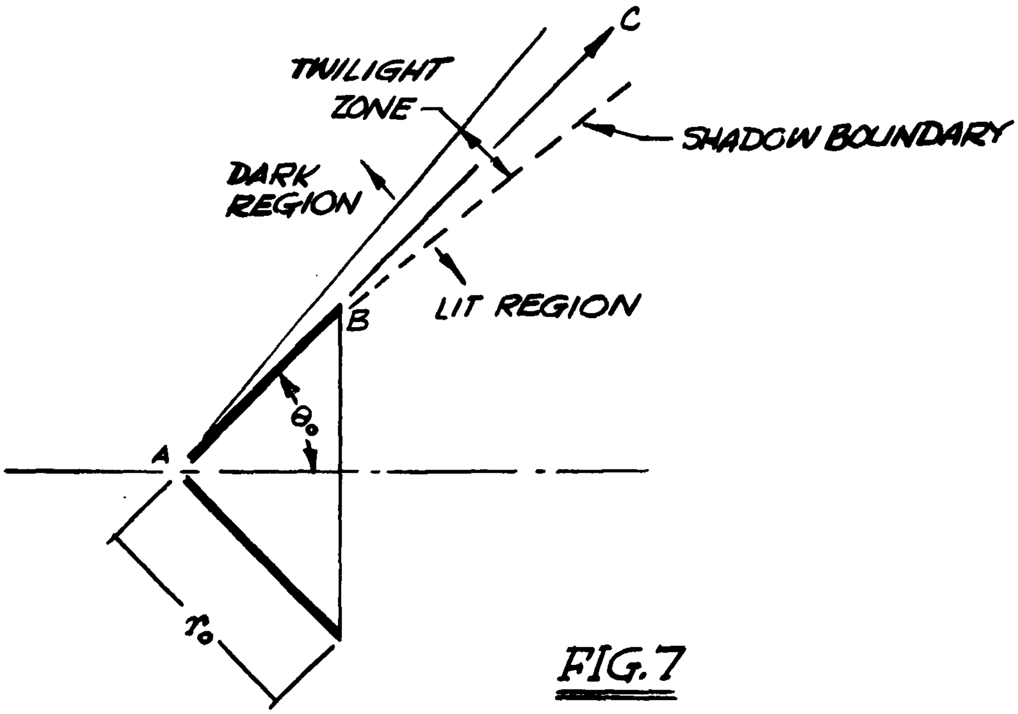

FIG.7

The distortion of the spherical phase front in the twilight zone is such as to correct for the spherical aberration in this region. Let us examine this quantitatively.

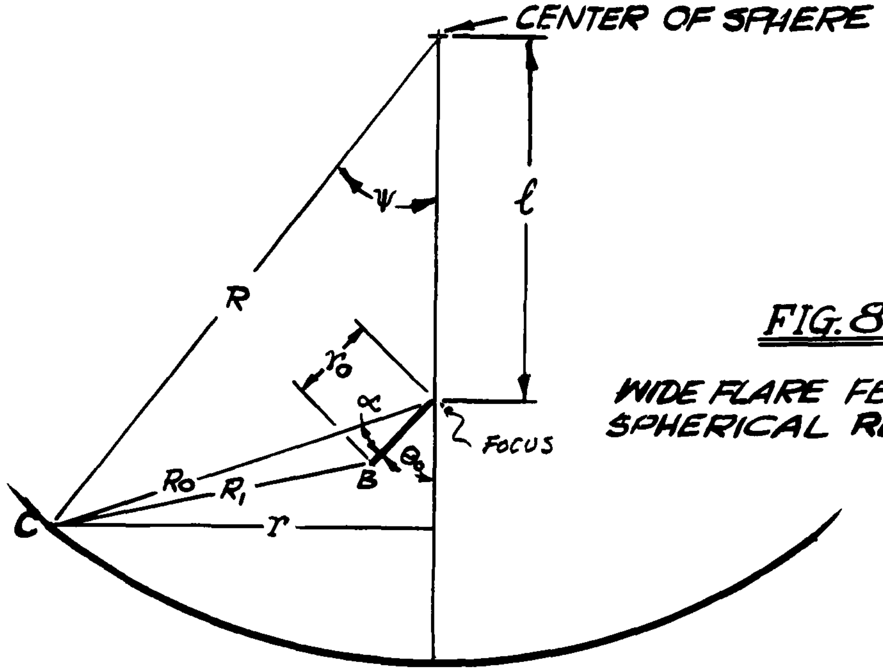

FIG. 8

WIDE FLARE FEED IN SPHERICAL REFLECTOR

From the geometry of Figure 8 we have

(47)

$$\psi = \sin^{-1}\left(\frac{r}{R}\right)$$

$$R_0 = \sqrt{R^2 + \ell^2 - 2R\ell\cos\psi}$$

$$\alpha = \sin^{-1}\left(\frac{r}{R_0}\right) - \theta_0$$

$$R_1 = \sqrt{R_0^2 + r_0^2 - 2R_0 r_0 \cos\alpha}$$

If α is less than zero, the ray from the focus to the general point C on the reflector is in the lit region and the phase error after reflection by the sphere is, as given in eq(25)

(48) $$\Delta_0 = R_0 - 2R + z + \ell \ , \quad z = R \cos\psi = \sqrt{R^2 - r^2} \ .$$

If α is greater than zero, the ray is in the twilight zone and the phase error after reflection by the sphere is

(49) $$\Delta_1 = r_0 + R_1 - R_0 + \Delta_0 .$$

In addition, a phase delay equivalent to an additional path length of $\lambda/8$ develops in the twilight zone. [3, p. 2] If we assume that this extra phase delay is proportional to $r_0 + R_1 - R_0$ throughout the twilight zone, the total phase error in the twilight zone becomes

(50) $$\Delta = \frac{5}{4}(r_0 + R_1 - R_0) + \Delta_0 .$$

This result agrees fairly well with some measured data (see Fig. 29, [2]). The correction term "$(5/4)(r_0 + R_1 - R_0)$" can be used to enlarge the first Fresnel zone. When this term exceeds $5\lambda/8$, however, the illumination is so low in magnitude that it is not effective in increasing the aperture area. Typically the E plane illumination in this case has dropped to 15-20db. The H plane illumination has dropped even further - to perhaps as much as 30db (see Figure 23-28, [2]).

but by proper mode excitation and control in the horn there is reasonable expectation that the H plane taper can be made as slight as the E plane taper. Therefore the first Fresnel zone should be enlarged no further than the point where

(51) $$\Delta_0 = -\frac{5\lambda}{8} .$$

If we solve this expression for z we obtain

(52) $$z = -\frac{5\lambda}{8} - 2\ell + 2R - \sqrt{(R-2\ell)^2 + \frac{5\ell\lambda}{4}} .$$

For the optimum feed position, ℓ is given by (44) and z becomes

(53) $$z \simeq R - \frac{\sqrt{\lambda R}}{2}\left[\sqrt{2} + \frac{3}{\sqrt{2}}\right], \quad \text{for } R >> \lambda.$$

This corresponds to a value of r given by

(54) $$r''' \simeq \lambda^{1/4}R^{3/4}\sqrt{\frac{5}{\sqrt{2}}} = 1.882\lambda^{1/4}R^{3/4} = 301.5\lambda^{1/4}, \text{ for } R>>\lambda.$$

The ratio

(55) $$\left(\frac{r'''}{r''}\right)^2 = \frac{\sqrt{2} + \frac{3}{\sqrt{2}}}{2\sqrt{2}} = .8\text{db}$$

is the possible increase in gain to be obtained by a properly designed wide flare horn. It is possible to choose r_0 and θ_0 in a number of ways so that the first Fresnel zone can actually have a radius as large as r'''. First of all, we require that when $r = r'''$

(56) $$r_0 + R_1 - R_0 = \frac{\lambda}{2}.$$

This implies that the point B of Figures 7 or 8 must lie on an ellipse with foci at A and C. Then we must require that the angle θ_0 is sufficiently large so that the maximum of Δ_0 (which equals $\lambda/2$, and occurs at $r = r''$) occurs when α is considerably less than zero. This will ensure that the maximum of Δ occurs also at $r = r''$ and has a value of $\lambda/2$. The value of θ_0 should be chosen no larger than necessary for this purpose as the aperture blocking increases with increasing θ_0.

This type of horn is a practical design with a good illumination taper for low spillover and broad bandwidth. The theoretical gains $G_{r'}$ and $G_{r''}$ can not be realized with practical feeds. Conventional horns which illuminate only the first Fresnel zone actually spillover and illuminate some of the higher Fresnel zones which subtract from their gain, but the well designed wide-flare horn has less spillover.[2] The wide flare horns shown in Figure 22 [2] were tested with a 69" radius, 10 foot aperture diameter spherical reflector over a 4 to 1 frequency band. The distance D between the center of the sphere and the point where the flare intersects the waveguide transmission line was determined for maximum gain. Resulting pattern data is shown in Table 1.

TABLE 1

Horn No.	Freq. kmc/s	Meas. Gain(db)	Width of Lobe (degrees) E plane	Width of Lobe (degrees) H plane	1st Sidelobes (db) E plane	1st Sidelobes (db) H plane	D (inches)	λ(inches)
1	8.338	39.	1.50	1.82	-20	-22	36.25	1.416
	8.535	38.9	2.0	1.6	-16	-24	35.63	1.383
	9.621	40.0	1.6	1.8	-20	-23	35.75	1.227
	24.0	47.9	.60	.80	-16	-16	36.0	492
	34.9	51.9	.57	.39	-12	-25*	36.0	338
2	8.338	38.2	1.80	1.85	-20	-20	34.75	
	8.535	37.8	1.8	1.9	-19	-22	35.31	
	9.621	39.3	1.3	1.8	-24	-22	35.63	
	24.0	47.5	.69	.78	-16	-18	35.4	
	34.[illegible]	51.9	47	.62	-15	-23*	35.6	
3	8.338	38.9	1.72	1.67	-20	-21	35.5	
	8.535	38.8	1.9	1.4	-17	-25	35.44	
	9.621	40.2	1.4	1.4	-25	-21	35.69	
	24.0	47.0	.81	.73	-20	-15	36.0	
	34.9	51.6	.40	.62	-14	-16	35.9	

* Widening of the main lobe indicated "swallowed" 1st sidelobes.

V- FOCUSSING OF SPILLOVER ENERGY

(a) General

In this section we apply the results of Section (II-b) to the analysis of focussing of spillover energy. The problem can be formulated in general terms as follows: If we are given a wavefront, such as the field produced by a feed, which illuminates a focussing device such as a lens or subdish of a Cassegrain system, there is also generally some energy which spills over or does not strike the focussing device. If the contour of the focussing device is parallel to a Fresnel zone boundary of the incident wavefront with respect to some field point P shadowed by the focussing device, this spillover field may have a considerable intensity at P. The situations of greatest interest usually occur when P is at the peak of the secondary beam.

Comparing (26) and (28), we see that the spillover field intensity at P is the intensity which would be present if the focussing device were removed, reduced by a factor which is the average illumination taper at the edge of the focussing device. For example, suppose a feed of nominal diameter D_f illuminates a lens of circular aperture and diameter D_b. Suppose that the gain of the feed alone and the feed with lens is respectively

$$(57) \qquad G_f = \eta_f\left(\frac{\pi D_f}{\lambda}\right)^2, \quad G_b = \eta_b\left(\frac{\pi D_b}{\lambda}\right)^2,$$

where η_f and η_b are the aperture efficiencies of the feed and of the feed and lens respectively. Then the power of the spillover energy relative to the total focussed energy in the peak direction in the far field is

(58) $$P_s = \frac{u_1^2 G_f}{G_b} = \frac{u_1^2 \eta_f}{\eta_b}\left(\frac{D_f}{D_b}\right)^2$$

where u_1 is the illumination taper at the edge of the lens of the incident feed energy as defined in (16).

For example, if the average illumination taper is 10db, and the gains of the feed and feed lens combination are respectively 12 and 23 db, then the spillover energy will be (23-12) + 10 = 21db below the peak energy of the main beam at the peak of the far field pattern.

Depending on the path difference, D between the lens-focussed and spillover energy, the signals could interfere constructively or destructively. Thus in the preceding example the spillover energy might add or subtract .6db to the gain as computed neglecting the spillover energy. Referring to Figure 9 the path difference D is $\overline{OAP'} - (\overline{OB} + \overline{BC} + \overline{CP})$ where BC is

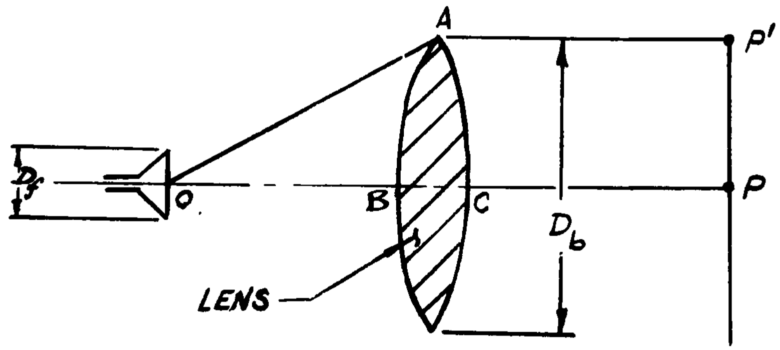

FIG. 9

the refractive index times the actual path length. D is likely to be large in wavelengths, so that whether spillover adds or subtracts from the gain would be frequency sensitive. The average illumination tap er may be obtained as the voltage average of the E and H plane tapers for typical "dipole mode"-type feeds. For example the 10db taper above might result from a 6db E plane taper and a 17.6db H plane taper.

If the observation point P is off the peak direction the directivity of the lens pattern and the spillover pattern reduce both signals. However the directivity pattern of the spillover energy being essentially that of a "ring source" is approximated by the Bessel function of order zero and has 7.4 db sidelobes. If the lens has zero thickness at A, this will not harm the overall sidelobe pattern otherwise, it can add new sidelobes at a level of about 21 + 7.4 = 28.4 db below peak. In addition, the sidelobes of the feed itself are har dly affected by the lens and will appear in the far field. For example in the E plane where normal feeds have about a 13db sidelobe level, one might expect (23-12) + 13 = 24db sidelobes. These lobes may occur at very large angles where normally much lower levels would be expected.

If the focussing device were a circular aperture reflector instead of a lens the spillover would cause a back lobe. Assuming for example, the same feed and the same antenna gain as in the previous example, the back lobe would be only 21 db below peak, whereas elsewhere on the backside of the reflector one would generally obtain much lower power levels, for example 30-50db. The feed thus puts a little bright spot centered on the dark side of the reflector.

Spillover focussing may be considerably reduced if the contour of the focussing device is not parallel to a Fresnel zone. If, for example, about one-half the contour coincides with one Fresnel zone boundary and the other half coincides with the boundary of the next Fresnel zone, the "bright spot" on the dark side can be made to vanish. If this is accomplished in some manner such as

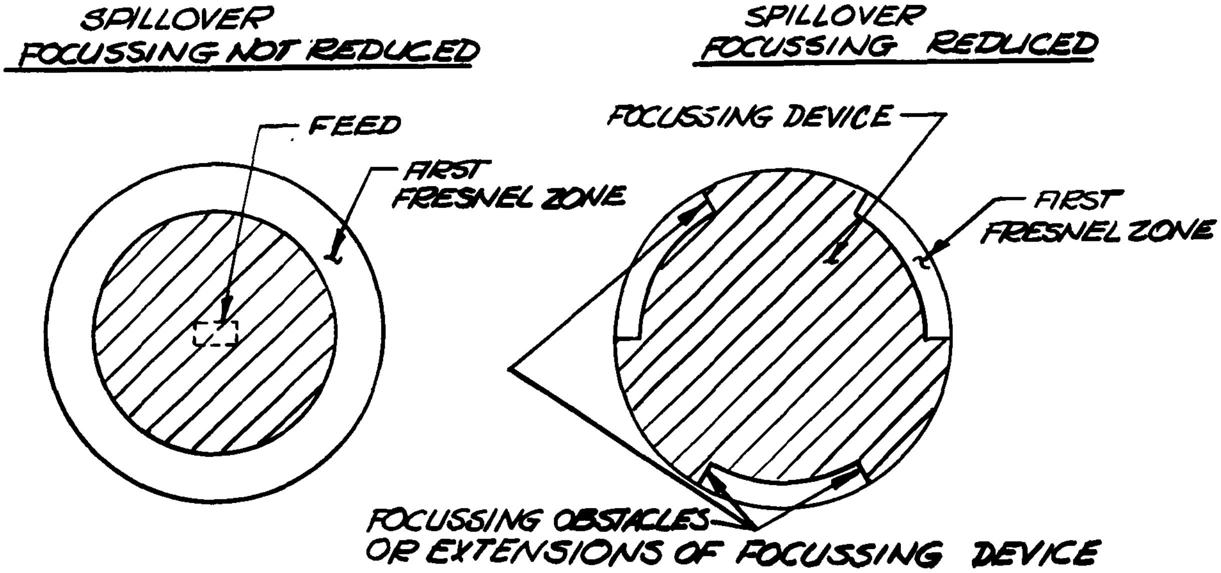

FIG. 10

shown in Figure 10 the spillover will not be well focussed even at a point nearby the focal point.

(b) Cassegrain Systems

From eq(58) it can be seen that the spillover energy becomes more important as the feed gain increases relative to the total antenna gain. In practical designs this situation occurs more frequently in a Cassegrain system. Typically a Cassegrain system is designed for "minimum blocking" - this is almost essential if the main reflector diameter D_m is less than 100 or 200λ. Minimum blocking occurs when the feed and subdish block equally. According to [6], in this case the diameter of the subdish D_b satisfies

$$D_b = \sqrt{\frac{2F_m\lambda}{k}} \tag{59}$$

where F_m is the focal length of the paraboloid, λ is the wavelength and k is a measure of the amplitude taper defined by

$$k = \frac{\lambda}{D_f\phi_s} \tag{60}$$

where ϕ_s is the half-angle subtended by the subreflector at the center of the feed aperture. In the H plane of typical feed horns for a 10db taper k equals or is slightly less than one and for a 20db taper k equals or is slightly less than one half. In the E plane, k is slightly larger.

In the minimum blocking design, the feed diameter D_f is proportional to the distance from the focus to the feed aperture plane, and may range from a nominal value of about one wavelength when the feed is close to the subdish to D_b itself when the feed is in the vertex plane of the main dish.

In the latter case the relative gain of the feed to the main dish is roughly equal to the ratio of $(D_b/D_m)^2$ and for a value of D_m of 50 to 100λ (using (59)) is typically 20-25db. Thus the effect on gain of the focussed spillover energy is of the same order of magnitude as in the preceding examples.

The effect on the antenna sidelobes is considerably different, however.

The main lobe of the radiation pattern of the spillover energy is about D_m/D_b times as broad as the main lobe of the total antenna pattern. Therefore the spill-over main lobe covers the first few sidelobes of the complete antenna and may add constructively or destructively with the highest such sidelobe depending critically on the frequency or exact geometry.

Usually in Cassegrain system design aperture blocking is a major design consideration while feed spillover is neglected. The latter may be as important as the former. The difference between the field strength of the unblocked and blocked energy is proportional to the relative area of the blocking subdish to the main dish.

(61)
$$2\left(\frac{D_b}{D_m}\right)^2$$

The factor 2 arises from an approximation of the aperture illumination taper by a quadratic which emphasizes the center region. From (58) the field strength of the spillover energy, in the case of the vertex feed ($D_f = D_b$), is

(62)
$$u_1 \frac{D_b}{D_m}$$

The latter is more important than the former if

(63)
$$u_1 > \frac{2D_b}{D_m} .$$

This is often the case

In the design for minimum blocking described in [6] and embodied in eq(39), the design taper of the subdish illumination is not specified. We conclude this section by suggesting a procedure for determining this taper in an optimum way. The blocking and spillover voltages of (61) and (62) are generally in a rapidly varying phase relationship with respect to frequency. The average total power in these two unwanted signals is then approximately

$$P_u = 4\left(\frac{D_b}{D_m}\right)^2 + u_1^{\,2}\left(\frac{D_f}{D_m}\right)^2 . \tag{64}$$

If we use a linear relation obtained by fitting the data mentioned in the definition of k in (60) we have roughly

$$u_1 = .4k - .06, \qquad .05 < u_1 < .3. \tag{65}$$

Also, if the angle subtended by the subdish is not large so that

$$\phi_s \simeq \tan \phi_s \tag{66}$$

then

$$k = \frac{2\lambda F_m}{D_b^{\,2}} , \tag{67}$$

From (65) and (67), (64) becomes

$$P_u = 4\left(\frac{D_b}{D_m}\right)^4 + \left(\frac{.8\lambda F_m}{D_b^{\,2}} - .06\right)^2 \left(\frac{D_f}{D_m}\right)^2 . \tag{68}$$

With D_f fixed, there is a value of D_b minimizing P_u. This is the minimum "blocking and spillover" design.

APPENDIX - OPTIMUM FEED AMPLITUDE PATTERN FOR MAXIMUM GAIN OF A BOUNDED WAVEFRONT SOURCE (SEE P. 11)

Let

$$R = \frac{M(u)\overline{M}(u)}{N(u^2)} \tag{A1}$$

where M and N are linear operators ($\overline{M}$ is the conjugate of M).

$$M(u) = \int_{\rho_1}^{\rho_2}\int_0^{2\pi} e^{-j\rho^2} u(\rho, \theta)\rho\, d\rho\, d\theta \tag{A2}$$

$$N(u^2) = \int_{\rho_1}^{\rho_2}\int_0^{2\pi} u^2(\rho, \theta)\rho\, d\rho\, d\theta$$

and from (21)

$$G = \frac{4AR}{\lambda^2(\rho_2{}^2 - \rho_1{}^2)} \quad . \tag{A3}$$

Suppose $u(\rho, \theta)$ is the function maximizing G and hence R also, then R will be stationary for small ϵ and arbitrary real functions $v(\rho, \theta)$. Accordingly the linear term in ϵ in

$$R(u + \epsilon v) = \frac{(M(u) + \epsilon M(v))(\overline{M}(u) + \epsilon \overline{M}(v))}{N(u^2 + 2\epsilon uv + v^2)} \tag{A4}$$

must vanish for all v.

This implies

$$\text{(A5)} \qquad \frac{\mathcal{R}e\left\{M(v)\overline{M(u)}\right\}}{N(uv)} = \frac{|M(u)|^2}{N(u^2)} = R(u).$$

Now let v be a Dirac delta function of (ρ, θ)

$$\text{(A6)} \qquad v = \delta(\rho_0, \theta_0).$$

(A5) reduces to

$$\text{(A7)} \qquad \frac{\mathcal{R}e\left\{e^{-j\rho_0^{\,2}}\rho_0 \int_{\rho_1}^{\rho_2}\int_0^{2\pi} e^{j\rho^2} u(\rho,\theta)\rho\, d\rho\, d\theta\right\}}{\rho_0 u(\rho_0, \theta_0)} = C$$

where C is a constant, independent of ρ_0 and θ_0. Accordingly $u(\rho_0, \theta_0)$ is independent of θ_0

$$\text{(A8)} \qquad u(\rho_0, \theta_0) = u(\rho_0) = \frac{1}{C}(D\cos\rho_0^{\,2} + B\sin\rho_0^{\,2})$$

where

$$\text{(A9)} \qquad D = 2\pi\int_{\rho_1}^{\rho_2} \cos\rho^2 u(\rho)\rho\, d\rho$$

$$B = 2\pi\int_{\rho_1}^{\rho_2} \sin\rho^2 u(\rho)\rho\, d\rho\,.$$

If we insert (A8) into (A9) we may evaluate C

(A10) $$C = \frac{\pi}{2}\left[\rho_2^{\,2} - \rho_1^{\,2} + |\sin(\rho_2^{\,2} - \rho_1^{\,2})|\right]$$

and obtain a linear relation between B and D

(A11) $$D = \frac{(\cos 2\rho_1^{\,2} - \cos 2\rho_2^{\,2})B}{2|\sin(\rho_2^{\,2} - \rho_1^{\,2})| + \sin 2\rho_1^{\,2} - \sin 2\rho_2^{\,2}}$$

unless the aperture contains an integral number of Fresnel zones

(A12) $$\rho_2^{\,2} = \rho_1^{\,2} + n\pi$$

in which case, B and D are independent and arbitrary. We also note that C is the optimum value of R(u) and the optimum gain from (A3) is

'A13) $$G = \frac{2\pi A}{\lambda^2}\left(1 + \frac{|\sin(\rho_2^{\,2} - \rho_1^{\,2})|}{\rho_2^{\,2} - \rho_1^{\,2}}\right).$$

We see therefore that when the aperture contains an integral number of Fresnel zones, the aperture efficiency is exactly 50%, otherwise it is larger. The maximum aperture efficiency for an aperture larger than one Fresnel zone is $1/2 + 1/3\pi = 60.5\%$, and occurs when $\rho_2^{\,2} = \rho_1^{\,2} + 3\pi/2$. In this case, the optimum illumination is

(A14) $$u(\rho, \theta) = \cos\rho^2 + \sin\rho^2.$$

The pattern of an average feed horn as given in Figure 5 of "Some Feed Horn Design Curves," by W. F. Gabriel, NRL Report, dated June 1951, was used to evaluate eq(21) for various aperture tapers. It was determined (Calculation 151-(14)) that for maximum gain the 20 db point of the illumination should be placed where the phase error is 176°. In this case the aperture efficiency over the area illuminated to the 20 db point will be 33.9% and the maximized gain will be

$$G = \frac{13.1}{\lambda\sqrt{\alpha\beta}} .$$

REFERENCES

[1] A. F. Kay, "A Line Source Feed for a Spherical Reflector," Contract AF19(604)-5532, dated May 29, 1961 (TRG Report No. 131).

[2] A. F. Kay, "The Wide Flare Horn - A Novel Feed for Low Noise Broadband and High Aperture Efficiency Antennas," Contract AF19(604)-8057, dated October 2, 1962 (TRG Report No. 151).

[3] J. B. Keller, R. M. Lewis, and B. D. Seckler, "Diffraction by an Aperture II," Journal of Applied Physics, 28, No. 5, May 1957, pp. 570-579.

[4] S. Silver, "Microwave Antenna Theory and Design," Rad Lab Series, Vol. 12, McGraw Hill, New York 1948.

[5] R. M. Searing, "An Analysis of Stationary Hemispherical Reflectors Used as Narrow-beam Wide Angle Scanning Antennas," Lockheed Missiles and Space Division LMSD-28805, November 1959.

[6] P. W. Hannan, "Microwave Antennas Derived from the Cassegrain Telescope," IRE Trans. AP-9 March 1961, pp. 140-153.

MASTER DISTRIBUTION LIST FOR ANTENNA LABORATORY

Note: One copy unless otherwise designated

Code	Organization
AF29	APGC (PGAPI) Eglin AFB, Florida
AF143	RADC (RCE) Attn/ Dr. John S. Burgess Griffiss AFB, New York
AF69	Director of Resident Training 3380th Technical Training Grp. Keesler AFB, Mississippi Attn/ OA-3011 Course
AF5	AF Missile Test Center Patrick AFB, Florida Attn/ AFMTC, Tech. Library, MU-135
AF227	USAF Security Service (CLR) San Antonio, Texas
AF166	Hq. USAF (AFOAC-S/E) Communications-Electronics Directorate, Washington, D C
AF231	Director, Electronics Div, Air Technical Intelligence Ctr. Attn/ AFCIN-4E1, Col. H.Gilbert Wright-Patterson AFB, Ohio
AF348	Lt. Col. Jensen (SSRTW) Space Systems Division Air Force Unit Post Office Los Angeles 45, California
Ar 47	Ballistic Research Labs. Aberdeen Proving Ground, Md. Attn/ Technical Inform. Branch
Ar 5	Commanding General, USASRDL Fort Monmouth, New Jersey Attn/ Tech. Doc. Center SIGRA/SL-ADT
AF124	RADC (RAYLD) Attn/ Documents Library Griffiss AFB, New York
AF139	AF Missile Dev. Center(MDGRT) Holloman AFB, New Mexico
AF86	SAC (Operations Analysis Office) Offutt AFB, Nebraska
AF18	AUL Maxwell AFB, Alabama
AF43	ASD (ASAPRD - Dist) Wright-Patterson AFB, Ohio
AF63	WADD (WCLRSA, Mr. Portune) Wright-Patterson AFB, Ohio
AF68	ASD (ASRNRE-3) Attn/Mr. Paul Springer Wright-Patterson AFB, Ohio
AF308	WADD (WWDRTR Mr. A. D. Clark) Directorate of System Engineer. Dyna Soar Engineering Office Wright-Patterson AFB, Ohio
Ar 42	Director U.S Army Ordnance Ballistic Research Laboratories Aberdeen Proving Ground, Md. Attn/ Ballistic Measurement Lab.
Ar 3	Director Evans Signal Laboratory Belmar, New Jersey Attn/ Mr O C Woodyard
AF253	Technical Information Office European Office, Aerospace Res Shell Building, 47 Cantersteen Brussels, Belgium

Code	Organization
M17	AFCRL Office of Aerospace Research (CRRD) Attn/ Contract Files L G Hanscom Field Bedford, Mass (2 copies)
M17	AFCRL Office of Aerospace Research (CRRD) Attn/ C J Sletten L G Hanscom Field Bedford Mass. (3 copies)
N3	Chief, Bureau of Ships Department of the Navy Washington 25 D. C Attn/ Code 690
N16	Commander U S Naval Air Missile Test Ctr. Point Mugu California Attn/ Code 366
N26	Commander U S Naval Ordnance Test Stat China Lake, California Attn/ Code 753
G126	National Aeronautics and Sp. Administration Attn/ Antenna Systems Br. Goddard Space Flight Center Greenbelt Maryland
N30	Dr. J I Bohnert Code 5210 U S Naval Research Lab. Washington 25 D C
N37	Chief of Naval Research Department of the Navy Washington 25 D C Attn/ Code 427
N73	Office of Naval Research Branch Office, London Navy 100 Box 39 F. P O. New York, New York
M54	Headquarters ESD (ESRDW, Major J. J Hobson) L G Hanscom Field Bedford Mass.
M59	Electronic Systems Division (AFSC), Technical Information Service Division (ESAT) L G Hanscom Field Bedford, Mass
M84	Headquarters, AFCRL OAR (CRXR, J.R. Marple) L. G. Hanscom Field Bedford, Mass.
N9	Chief Bureau of Naval Weapons Department of the Navy Washington 25 D C Attn/ DLI-31 (2 copies)
N23	U S Naval Ordnance Laboratory White Oak, Silver Spring 19, Md. Attn/ The Library
N27	Librarian U S Naval Postgraduate School Monterey, California
N29	Director U S Naval Research Laboratory Washington 25, D C Attn/ Code 2027 (2 copies)
N35	Commanding Officer and Dir. U S Navy Underwater Sound Lab. Fort Trumbull, New London, Connecticut
N48	Commanding Officer U S Naval Air Development Ctr. Johnsville Penna Attn/ NADC Library
N85	Commanding Officer and Dir. U S Navy Electr Lab (Library) San Diego 52, California

Code	Organization
Ar 10	Mass. Institute of Technology Signal Corps Liaison Officer Cambridge 39, Mass. Attn/ A Bedrosian, Rm26-131
Ar 49	Commanding General USASRDL Fort Monmouth, New Jersey Attn/SIGFM/EL-AT
AR67	Redstone Scientf. Info. Ctr. U.S. Army Missile Command Redstone Arsenal, Alabama
Ar 41	Office of Chief Signal Officer Engineering and Tech. Div. Washington 25, D C Attn/ SIGNET-5
AF33	AFOSR, OAR (SRYP) Tempo D 4th and Independence Ave. Washington 25, D C.
G103	National Aeronautical Sp Agcy Langley Aeronautical Res. Lab Langley Virginia Attn/ Cliff Nelson
G13	National Bureau of Standards U S Department of Commerce Washington 25 D C Attn/ Mr A G McNish
G75	Director National Security Agency Fort Meade Maryland Attn/ C3/TDL
M6	AFCRL, OAR(CRXRA-Stop 39) L. G. Hanscom Field Bedford, Mass. (10 copies) (ship separately from other AFCRC copies)
Ar 78	Commanding General, SIGFM/EL-PC USASRDL Fort Monmouth New Jersey Attn/ Dr. H K Kedesdy Deputy Chief, Chem Physics Br.
Ar 39	Commanding General USASRDL Fort Monmouth, New Jersey Attn/ Mr. F J Triola
Ar 9	Department of the Army Office of the Chief Signal Officer Washington 25 D C Attn/ SIGRD-4a-2
Ar 48	Guided Missile Fuze Library Diamond Ordnance Fuze Labs. Washington 25, D C Attn/ R D Hatcher, Chief Microwave Development Section
G 2	ASTIA (TIPAA) Arlington Hall Station Arlington 12, Virginia (10 copies)
G 8	Library National Bureau of Standards Boulder Laboratories Boulder, Colorado (2 copies)
G27	National Bureau of Standards U S Department of Commerce Washington 25, D C Attn/ Gustave Shapiro, Chief Engineering Electronics Section Electricity and Electr Division
G9	Defense Research Member Canadian Joint Staff 2450 Mass Ave., NW Washington 8, D C

Code	Organization
N91	Commander U S Naval Air Test Ctr Patuxent River, Maryland Attn/ ET-315, Antenna Br
N93	Commanding Officer U S Naval Ordnance Lab. Corona, California Attn/ Documents Librarian
N141	AFSC Scientific and Tech. Liaison Office, c/o Department of the Navy Room 2305, Munitions Bldg Washington 25, D. C
I940	Aerospace Corporation Box 95085 Los Angeles 45, California Attn/ Library
I388	Aircom, Inc. 48 Cummington Street Boston Mass.
I374	ACF Electr. Division Bladensburg Plant 52nd Ave, and Jackson St. Bladensburg, Maryland Attn/ Librarian Attn/ Librarian
I8	Bell Aircraft Corporation Post Office Box One Buffalo 5, New York Attn/ Eunice P Hazelton, Libr
I246	Bendix Corporation Pacific Division 11600 Sherman Way North Hollywood, California Attn/ Engineering Library
I248	Bjorksten Res. Labs, Inc. P O Box 265 Madison, Wisconsin Attn/ Librarian
N92	Material Lab., Code 932 New York Naval Shipyard Brooklyn 1, New York Attn/ Mr Douglas First
N123	Chief, Bureau of Ships Department of the Navy Washington 25, D C Attn/ Code 817B
I601	Aero Geo Astro Corp. 1200 Duke Street Alexandria, Virginia Attn/ Library
I1	Airborne Instruments Lab. Inc. Division of Cutler Hammer Walt Whitman Road Melville, L I, New York Attn/ Library
I3	Andrew Alford Conulsting Engr 299 Atlantic Avenue Boston10, Mass
I205	Battelle Memorial Institute 505 King Avenue Columbus 1, Ohio Attn/ Wayne E Rife, Proj. Ldr. Electrical Engineering Division
I469	Bell Telephone Laboratories Murray Hill, New Jersey
I13	Bell Telephone Laboratories Whippany Laboratory Whippany, New Jersey Attn/ Technical Information Libr.
I247	Bendix Radio Division Bendix Aviation Corporation E Joppa Road Towson 4, Maryland Attn/ Dr. D M Allison, Jr., Dir. Engineering and Research

Code	Organization
1249	Boeing Airplane Company Pilotless Aircraft Division P O Box 3707 Seattle 24. Washington Attn/ R R Barber, Library
1252	Brush Beryllium Company 4301 Perkins Avenue Cleveland 3, Ohio Attn/ N W Bass
1986	Chance Vought Corporation Vought Electronics Division P O Box 5907 Dallas 22 Texas
1918	Collins Radio Company 855 35th Street NE Cedar Rapids. Iowa Attn/ Dr. R L. McCreary
125	Cornell Aeronautical Lab. Inc. 4455 Genesee Street Buffalo 21. New York Attn: Librarian
1255	Dalmo Victor Company A Division of Textron. Inc. 1515 Industrial Way Belmont. California Attn/ M E Addoms. Libr
1258	Douglas Aircraft Company 3000 Ocean Park Blvd. Santa Monica, California Attn/ P. Duyan Jr., Chief Electr. Electronics Section
1259	Douglas Aircraft Company 2000 North Memorial Drive Tulsa. Oklahoma Attn/ Engr Librarian, D250
1415	Electronics Communication 1830 York Road Timonium. Maryland

Code	Organization
1250	Boeing Airplane Company Wichita Division Engr. Library Wichita 1. Kansas Attn/ K C Knight, Libr. Superv.
1253	Chance Vought Aircraft, Inc. 9314 West Jefferson Street Dallas, Texas Attn/ A. D Pattullo, Librarian
1470	Chu Associates P O Box 387 Whitcomb Avenue Littleton. Mass.
1126	Convair, A Division of General Dynamics Corporation Fort Worth, Texas Attn/ K. G Brown. Div. Res. Libr.
1254	Convair. A Division of General Dynamics Corporation 3165 Pacific Highway San Diego 12, California Attn/ Mrs. D B Burke, Libr.
128	Dorne and Margolin. Inc. 29 New York Avenue Westbury. L I , New York
1257	Aircraft Division Douglas Aircraft Company, Inc. 3855 Lakewood Blvd. Long Beach, California Attn/ Tech. Library
1145	The Electrada Corporation 11244 Playa Street Culver City, California Attn/ S. S. Locus, Section Head Microwave Engineering
1187	Electromagnetic Research Corp. 5001 College Ave. College Park, Maryland Attn/ Mr. Martin Katzin

Code	Organization
1207	Hughes Aircraft Company Antenna Department Building 12, Mail Station 2714 Culver City, California Attn/ Dr. W. H Kummer
1981	Hughes Aircraft Company Attn/ Mr. L Stark, Micro. Dept Radar Laboratory P. O. 2097 Building 600, Mail Sta. C-152 Fullerton. California
1414	International Resistance Co. 401 N. Broad Street Philadelphia 8 Penna. Attn/ Research Library
1230	Jansky and Bailey Inc. 1339 Wisconsin Ave., NW Washington 7, D. C Attn/ Mr. D. C Ports
1279	Lockheed Aircraft Corp. 2555 N. Hollywood Way California Div. Engr. Libr. Dept. 72-25, Plant A 1 Build. 63-1 Burbank, California Attn/ N. C. Harnois
1136	The Martin Company P O Box 179 Denver 1 Colorado Attn/ Mr. J. McCormick
163	Mathematical Reviews 190 Hope Street Providence 6 R. I
1282	McDonnell Aircraft Corp. Dept. 644 Box 516. St. Louis 66 Missouri Attn/ C. E Zoller, Engr. Libr

Code	Organization
156	Hughes Aircraft Company Florence Ave. and Teale Street Culver City, California Attn/ L L. Bailin. Manager Antenna Department
1302	International Business Mach. Corp. Space Guidance Center - Federal Systems Division Owego, Tioga County, NY Attn/ Tech. Report Center
1265	ITT Laboratories 3700 East Pontiac Street Fort Wayne 1, Indiana Attn/ Technical Library
1241	Dr. Henry Jasik Consult. Engr. 298 Shames Drive Brush Hollow Industr. Park Westbury, New York
1468	Lockheed Aircraft Corporation Missiles and Space Division Tech. Information Center 3251 Hanover Street Palo Alto, California (2 copies)
1280	The Martin Company Baltimore 3 Maryland Attn/ Engineering Library Antenna Design Group
166	The W L Maxson Corp. 475 10th Avenue New York. New York Attn/ Miss Dorothy Clark
1283	McMillan Laboratory, Inc. Brownville Avenue Ipswich Mass. Attn/ Sec. Officer, Doc. Rm.

Code	Organization
1299	Electronic Specialty Company 5121 San Fernando Road Los Angeles 39. California Attn/ D L Margerum, Chief Engr., Rad. Syst. Div.
1147	Emerson Radio-Phonograph Emerson Research Labs. 701 Lamont Street, NW Washington 10. D C Attn/ Mrs. R Corbin. Libr
1266	ITT Federal Laboratories Technical Library 500 Washington Avenue Nutley 10, New Jersey
14	Gabriel Electronics Division Main and Pleasant Streets Millis. Mass. Attn/ Dr. Edw. Altshuler
1793	General Electric Company Missile and Space Vehicle Dept 3198 Chestnut Street. Philadelphia. Penna. Attn/ Documents Library
1270	General Precision Lab, Inc. 63 Bedford Road Pleasantville. New York Attn/ Librarian
1448	Granger Associates Electronic Systems 974 Commercial Street Palo Alto. California Attn/ J V N Granger, Pres.
1737	The Hallicrafters Co. 5th and Kostner Avenues Chicago 24. Illinois Attn/ H. Hodara Head Space Communication

Code	Organization
1204	Emerson and Cuming, Inc. 869 Washington Street Canton. Mass Attn/ Mr. W. Cuming
1262	Emerson Electric Mfg. Co. 8100 West Florissant Ave St. Louis 21, Missouri Attn/ E R Breslin, Librarian
1264	Fairchild Aircraft-Missiles Div. Fairchild Engr and Airplane Corp. Hagerstown, Maryland Attn/ Library
1269	General Electric Company Electronics Park Syracuse, New York Attn/ Doc. Library. Bldg 3-143A B Fletcher
1893	General Electric Company 3750 D Street Philadelphia 24. Penna. Attn/ Mr. H. G Lew Missile and Space Veh. Dept.
148	Goodyear Aircraft Corp. 1210 Massillon Road Akron 15. Ohio Attn/ Library, Plant G
1272	Grumman Aircraft Engr Corp. Bethpage, L. I., New York Attn/ Engr. Librarian. Plant 5
1273	Hallicrafters Company 4401 West 5th Avenue Chicago 24. Illinois Attn/ LaVerne LaGioia, Libr.
1274	Hoffman Electronics Corp. 3761 South Hill Street Los Angeles 7, California Attn/ Engr. Library

Code	Organization
1116	Melpar, Inc. 3000 Arlington Boulevard Falls Church, Virginia Attn/ Engr. Tech Libr
1390	Microwave Develop. Lab. 90 Broad Street Wellesly 57. Mass Attn/ N. Tucker, Gen. Mgr.
185	Motorola. Inc. 8201 East McDowell Road Phoenix, Arizone Attn/ Dr. T E. Tice
1285	North American Aviation Inc. Los Angeles International Airport Los Angeles 45, California Attn/ Engr. Tech. File
1286	Page Communications Engr. Inc. 2001 Wisconsin Ave., NW Washington 7, D C Attn/ Mrs. R Temple, Libr.
1287	Philco Corporation Research Division Union Meeting Pond Blue Bell. Penna. Attn/ Research Librarian
1288	Polytechnic Res. and Dev. Co., Inc. 202 Tillary Street Brooklyn 1, New York Attn/ Tech. Library
1289	Radiation, Inc Melbourne, Florida Attn/ RF Systems Div. Technical Information Ctr.
1290	RCA Laboratories David Sarnoff Research Ctr. Princeton, New Jersey Attn/ Miss F Cloak, Libr.

Code	Organization
1471	Microwave Associates, Inc. South Avenue Burlington, Mass
1648	The Mitre Corporation 244 Wood Street Lexington 73, Mass. Attn/ Mrs. J Claflin, Libr
1641	National Research Council Radio and Electr Engr. Div. Ottawa, Ontario, Canada Attn/ Dr. G A Miller, Head Microwave Section
1284	North American Aviation, Inc 12214 Lakewood Blvd. Downey, California Attn/ Tech Information Ctr. (495-12) Space and Infor. Sys. Div.
182	Northrop Corporation Norair Division 1001 East Broadway Hawthorne, California Attn/ Tech. Inform. 3924-31
1225	Pickard and Burns, Inc. 103 Fourth Avenue Waltham 54. Mass. Attn/ Dr. R H Woodward
1232	Radiation Engineering Lab. Main Street Maynard. Mass. Attn/ Dr. John Ruze
1914	Radiation Systems, Inc 440 Swann Avenue Alexandria, Virginia Attn/ Library
1291	Radio Corporation of America Defense Electronic Products Bldg. 10, Floor 7 Camden 2, New Jersey Attn. H. J Schrader, Staff Engr. Organization of Chief Tech. Adm.

Code	Organization
I473	Radio Corporation of Amer. Missile Contrl and Electr. Div. Bedford Street Burlington, Mass. Attn/ Librarian
I789	Radio Corporation of Amer. West Coast Missile and Surf. Radar Division Engineering Libr . Bldg. 306/2 Attn/ L. R. Hund, Librarian 8500 Balboa Boulevard Van Nuys, California
I292	Director, USAF ProjRAND Via: AF Liaison Office The Rand Corporation 1700 Main Street Santa Monica, California
I293	Raytheon Company State Road, Wayland Lab. Wayland, Mass. Attn/ Mr. Robert Borst
I472	Raytheon Company Missile Systems Division Hartwell Road Bedford, Mass. Attn/ D. H. Archer
I295	Republic Aviation Corp. Farmingdale, L. I., N Y Attn/ Engr. Library Via AF Plant Representative
I391	Sage Laboratories, Inc. 3 Huron Drive Natick, Mass.
I96	Sandia Corporation P. O. Box 5800 Alburquerque, New Mexico Attn/ Records Mgt. and Serv Dept.

Code	Organization
I757	Radio Corporation of America Surface Communic. Syst. Lab 75 Varick Street New York 13, New York Attn/ Mr. S. Krevsky
I930	Radio Corporation of America Defense Electr. Products Advanced Military Systems Princeton, New Jersey Attn/ Mr. David Shore
I547	The Rand Corporation 1700 Main Street Santa Monica, California Attn/ Technical Library
I373	Rantec Corporation 23999 Ventura Boulevard Calabasas, California Attn/ Grace Keener, Office Mgr.
I294	Raytheon Company Wayland Laboratory Wayland, Mass. Attn/ Miss A. Anderson, Libr.
I510	Remington Radn UNIVAC Division of Sperry Rand Corp. P O. Box 500 Blue Bell, Pa. Attn/ Engr. Library
I184	Ryan Aeronautical Company 2701 Harbor Drive Lindbergh Field San Diego 12, California Attn/ Library
I142	Sanders Associates, Inc. 95 Canal Street Nashua, New Hampshire Attn/ N. R Wild

Code	Organization
U3	Space Sciences Laboratory Leuschner Observatory University of California Berkely 4, California Attn/ Dr. S Silver, Director
U289	University of S California University Park Los Angeles, California Attn/ Dr. R. L. Chuan, Dir.
U183	Columbia University Dept. of Electr Engr. Morningside Hghts, NY, NY Attn/ Dr Schlesinger
U10	Cornell University School of Electr. Engr. Ithaca, New York Attn/ Prof. G. C Dalman
U59	Georgia Tech. Res. Inst. Engr Experiment Station 722 Cherry Street NW Atlanta, Georgia Attn/ Mrs. H H. Crosland Librarian (Unclassified)
U54	Harvard College Observ. 60 Garden Street Cambridge 39, Mass. Atn/ Dr. F. L Whipple
U104	University of Illinois College of Engineering Urbana, Illinois Attn/ Dr. P. E Mayes, E. E.
U240	Illinois Institute of Tech. Technology Center Dept. of Electr. Engr. Chicago 16, Illinois Attn/ P. C. Yuen, Electr. Res. Laboratory

Code	Organization
U100	University of California Electronics Research Lab. 332 Cory Hall Attn/ J R Whinnery
U239	Case Institute of Tech. Electrical Engr. Department 10900 Euclid Ave. Cleveland, Ohio Attn/ Prof. Robert Plonsey
U238	Unversity of S. California University Park Los Angeles 7, California Attn/ A. Kaprielian, Assoc. Prof.
U86	University of Florida Dept. of Electr. Engr. Gainesville, Florida Attn/ Prof. M H. Latour, Libr.
U102	Harvard University Tech. Report Collection Gordon McKay Library 303 Pierce Hall Oxford Street Cambridge 38, Mass.
U103	University of Illinois Documents Divis. Library Urbana, Illinois (Unclassified)
U169	Illinois Institute of Tech. 3301 S Dearborn St. Chicago 16, Illinois Attn/ Dr. G I Cohn
U22	The John Hopkins University Homewood Campus Baltimore 18, Maryland Attn/ Dr. D. E. Kerr, Phys. Dept.

Code	Organization
I682	Scanwell Laboratories, Inc. 6601 Scanwell Lane Springfield, Virginia
I297	Sperry Cyroscope Company Great Neck, L. I., New York Attn/ F W Turnbull, Engr. Libr.
I367	Stanford Research Institute Documents Center Menlo Park, California Attn/ Acquisitions
I260	Sylvania Electric Prod Inc. Electronic Defense Lab. P O Box 205 Mountain View, California Attn/ Library
I338	A S Thomas, Inc 355 Providence Highway Westwood Mass. Attn/ A S Thomas, Pres.
I708	Texas Instruments, Inc 6000 Lemmon Avenue Dallas 9, Texas Attn/J. B Travis. Systems Planning Branch
U1	Library Geophysical Inst. of the University of Alaska College, Alaska
U61	Brown University Department of Elect Engr. Providence, R I Attn/ Dr. C M Angulo
U99	California Institute of Tech. 1201 E. California Street Pasadena, California Attn/ Dr. C. Papas

Code	Organization
I312	STL Technical Library Document Acquisitions Space Technology Labs Inc P O Box 95001 Los Angeles 45, California
I934	Motorola, Inc Phoenix Res. Laboratory 3102 N 56th Street Phoenix, Arizona Attn/ Dr. A. L Aden
I104	Sylvania Electric Prod. Inc 100 First Avenue Waltham 54 Mass. Attn/ C A Thornhill, Libr Waltham Labs, Library
I818	Sylvania Reconnaissance Sys. Lab Box 188 Mountain View California Attn/ Marvin D Waldman
I464	Trans-Tech, Inc P O Box 346 Rockville, Maryland Attn/ A C Blankenship, Chief Electronics Engineer
I139	Westinghouse Electric Corp. Electronics Division Friendship International Airp. Box 1897 Baltimore 3, Maryland Attn/ Engineering Library
U157	California Inst. of Technology Jet Propulsion Laboratory 4800 Oak Grove Drive Pasadena, California Attn/ I. E. Newlan

Code	Organization
U105	The John Hopkins University Applied Physics Laboratory 8621 Georgia Avenue Silver Springs, Maryland Attn/ Mr. George L Seielstad
U68	Lowell Technological Institute Research Foundation P O Box 709 Lowell Mass. Attn/ Dr C R Mingins
U34	McGill University Dept of Electrical Engineering Montreal, Canada Attn/ Dr T Pavlasek
U107	University of Michigan Electronic Defense Group Engineering Research Institute Ann Arbor, Michigan Attn/ J A Boyd, Supv.
U37	University of Michigan Engineering Research Institute Willow Run Labs. Ypsilanti Michigan Attn/ Librarian
U39	New York University Institute of Math Sciences Room 802, 25 Waverly Place New York 3, New York Attn Dr. Morris Kine
U43	Antenna Laboratory Dept. of Electrical Engineering The Ohio State University 2024 Neil Avenue Columbus 10, Ohio Attn. Librarian - Reports

Code	Organization
U228	University of Kansas Electrical Engineering Depart Lawrence, Kansas Attn/ Dr H Unz
U32	Mass Institute of Technology RLE, Blg 26, Room 327 Cambridge 39 Mass Attn/ John H Hewitt
U26	Mass. Institute of Technology Lincoln Laboratory P O Box 73 Lexington 73 Mass Attn/ M Granese Librarian
U79	University of Michigan Engineering Research Institute Radiation Laboratory 912 N. Main Street Ann Arbor, Michigan Attn/ Mr Ralph E Hiatt
U108	University of Minnesota Minneapolis 14, Minnesota Attn/ Mr. R H Stumm, Libr.
U194	Physical Science Laboratory New Mexico State University University Park New Mexico Attn/ Mr. H W Haas
U96	Northwestern University Microwave Labs Evanston, Illinois Attn/ R E Beam
U109	The University of Oklahoma Research Institute Norman, Oklahoma Attn/ Prof. C L Farrar, E E

Code	Organization
AF32	OAR (RROS, Col. J. Fowler Tempo D 4th and Independence Ave. Washington 25, D. C.
U48	Polytechnic Institute of Brooklyn Microwave Res. Institute 55 Johnson Street Brooklyn, New York Attn/ Dr. A. A. Oliner
U184	Purdue University Dept. of Electr. Engineering Lafayette Indiana Attn/ Dr. Schultz
U110	Syracuse University Res. Inst. Collendale Campus Syracuse 10, New York Attn/ Dr. C. S. Grove, Jr.
U186	University of Tennessee Ferris Hall W Cumberland Ave. Knoxville 16, Tennessee
U51	The University of Texas Defense Research Lab. Austin, Texas Attn/ C. W. Horton, Phys. Lib.
U133	University of Washington Dept. of Electr. Engineering Seattle 5, Washington Attn/ D K Reynolds
U361	The Pennsylvania State Univ. 223 Electr. Engineering University Park, Penna. Attn/ A. H. Waynick, Dir. Ionosphere Res. Lab.
G31	Office of Scientific Intelligence Central Intelligence Agency 2430 E St, NW Washington 25, D. C.

Code	Organization
U185	University of Pennsylvania Institute of Cooperative Res. 3400 Walnut Street Philadelphia, Penna Attn. Dept. of Electr Engr.
U97	Polytechnic Institute of Brooklyn Microwave Research Institute 55 Johnson Street Brooklyn, New York Attn/ A. E Laemmel
U176	Library W W. Hansen Laboratory of Phys. Stanford University Stanford, California
U309	Technical University Oestervoldgade 10G Copenhagen, Denmark Attn/ Prof. Hans L. Knudsen
U111	The University of Texas Electrical Engr. Res. Lab. P O. Box 8026, University Station Austin 12, Texas Attn/ J. R. Gerhardt, Asst. Dir.
U132	University of Toronto Dept. of Electr. Engineering Toronto, Canada Attn/ Prof. G. Sinclair
U187	University of Wisconsin Dept. of Electr. Engineering Madison, Wisconsin Attn/ Dr. Scheibe
AF314	HQ OAR (RROSP, Maj. Nelson) Tempo D 4th and Independence Ave. Washington 25, D. C.

AD Div. 8/2

TRG, Inc., East Boston, Mass.
APPLICATION OF FRESNEL ZONE THEORY TO MICROWAVE ANTENNA DESIGN by Alan F. Kay. Scientific Report November 15, 1962, 40 p. incl. illus. (Rept. No. 151-3) Contract AF19(604)8057
Unclassified report

Some fundamental formulas are derived which are corrections to geometrical optics for radiation from bounded wavefronts. These formulas apply in both the near and far field, in focal and caustic regions, and in lit, twilight, and dark zones. Applications are made to improving the gain of a spherical reflector and the analysis of (generally unwanted) focussing of spillover energy in microwave systems.

Earlier applications were in the design of low noise feeds and line source feeds for spherical reflectors.

UNCLASSIFIED

1. Microwave Optics
2. Antenna Radiation Patterns - Theory
3. Antennas Theory
I. Alan F. Kay
II. Electronic Systems Division
Air Force Systems Command
Office of Aerospace Research
Laurence G. Hanscom Field
Bedford, Massachusetts
III. Contract AF19(604)-8057

UNITERMS

Fresnel Zones
Physical Optics
Wavefronts

Armed Services Technical Information Agency
UNCLASSIFIED

AD Div. 8/2

TRG, Inc., East Boston, Mass.
APPLICATION OF FRESNEL ZONE THEORY TO MICROWAVE ANTENNA DESIGN by Alan F. Kay. Scientific Report November 15, 1962, 40 p. incl. illus. (Rept. No. 151-3) Contract AF19(604)8057
Unclassified report

Some fundamental formulas are derived which are corrections to geometrical optics for radiation from bounded wavefronts. These formulas apply in both the near and far field, in focal and caustic regions, and in lit, twilight, and dark zones. Applications are made to improving the gain of a spherical reflector and the analysis of (generally unwanted) focussing of spillover energy in microwave systems.

Earlier applications were in the design of low noise feeds and line source feeds for spherical reflectors.

UNCLASSIFIED

1. Microwave Optics
2. Antenna Radiation Patterns - Theory
3. Antennas Theory
I. Alan F. Kay
II. Electronic Systems Division
Air Force Systems Command
Office of Aerospace Research
Laurence G. Hanscom Field
Bedford, Massachusetts
III. Contract AF19(604)-8057

UNITERMS

Fresnel Zones
Physical Optics
Wavefronts

Armed Services Technical Information Agency
UNCLASSIFIED

AD Div. 8/2

TRG, Inc., East Boston, Mass.
APPLICATION OF FRESNEL ZONE THEORY TO MICROWAVE ANTENNA DESIGN by Alan F. Kay. Scientific Report November 15, 1962, 40 p. incl. illus. (Rept. No. 151-3) Contract AF19(604)8057
Unclassified report

Some fundamental formulas are derived which are corrections to geometrical optics for radiation from bounded wavefronts. These formulas apply in both the near and far field, in focal and caustic regions, and in lit, twilight, and dark zones. Applications are made to improving the gain of a spherical reflector and the analysis of (generally unwanted) focussing of spillover energy in microwave systems.

Earlier applications were in the design of low noise feeds and line source feeds for spherical reflectors.

UNCLASSIFIED

1. Microwave Optics
2. Antenna Radiation Patterns - Theory
3. Antennas Theory
I. Alan F. Kay
II. Electronic Systems Division
Air Force Systems Command
Office of Aerospace Research
Laurence G. Hanscom Field
Bedford, Massachusetts
III. Contract AF19(604)-8057

UNITERMS

Fresnel Zones
Physical Optics
Wavefronts

Armed Services Technical Information Agency
UNCLASSIFIED

AD Div. 8/2

TRG, Inc., East Boston, Mass.
APPLICATION OF FRESNEL ZONE THEORY TO MICROWAVE ANTENNA DESIGN by Alan F. Kay. Scientific Report November 15, 1962, 40 p. incl. illus. (Rept. No. 151-3) Contract AF19(604)8057
Unclassified report

Some fundamental formulas are derived which are corrections to geometrical optics for radiation from bounded wavefronts. These formulas apply in both the near and far field, in focal and caustic regions, and in lit, twilight, and dark zones. Applications are made to improving the gain of a spherical reflector and the analysis of (generally unwanted) focussing of spillover energy in microwave systems.

Earlier applications were in the design of low noise feeds and line source feeds for spherical reflectors.

UNCLASSIFIED

1. Microwave Optics
2. Antenna Radiation Patterns - Theory
3. Antennas Theory
I. Alan F. Kay
II. Electronic Systems Division
Air Force Systems Command
Office of Aerospace Research
Laurence G. Hanscom Field
Bedford, Massachusetts
III. Contract AF19(604)-8057

UNITERMS

Fresnel Zones
Physical Optics
Wavefronts

Armed Services Technical Information Agency
UNCLASSIFIED